Lab 2: Computational Approaches to Quantum Systems and Relativistic Motion

Umi Yamaguchi
October 14, 2024

Background

This lab explores three main areas: Quantum Harmonic Oscillators, the motion of a relativistic particle on a spring, and numerical differentiation. These topics allow us to investigate complex physical phenomena through computational approaches, such as numerical integration, Gaussian quadrature, and finite difference approximations for derivatives. The report is divided into three sections corresponding to these themes, with each section addressing multiple questions related to the topic.

1. Quantum Harmonic Oscillator

The quantum harmonic oscillator is a fundamental model in quantum mechanics, describing a particle oscillating in a potential well. The wavefunctions for different energy levels are constructed using Hermite polynomials, which characterize the shape of the wave at each level. Additionally, the potential energy is determined by calculating the expectation value of the position operator squared, $\langle X^2 \rangle$, using Gaussian quadrature.

a) Hermite Polynomial Function Implementation

We implemented $H(n, x)$ to compute the Hermite polynomials recursively. The recursion relation used is:
$H_{n+1}(x) = 2xH_n(x) - 2nH_{n-1}(x)$

where $H_0(x) = 1$ and $H_1(x) = 2x$.

b) Wavefunctions Plot

The wavefunctions $\psi_n(x)$ for $n = 0, 1, 2,$ and 3 were plotted over the interval $x \in [-4, 4]$. The plot reveals that as the energy level n increases, the wavefunctions become more oscillatory, with additional nodes indicating higher energy states. These oscillations reflect the quantum mechanical nature of the oscillator, where each state has a unique energy and probability distribution.

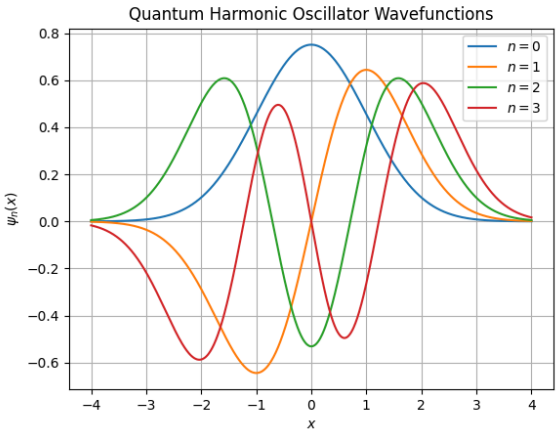

c) Potential Energy Calculation

The potential energy for the oscillator, represented by $\langle X^2 \rangle$, was computed using Gaussian quadrature. The integration was performed for n ranging from 0 to 10. The calculated values show a linear relationship between energy levels and the expectation value:

n = 0, $\langle X^2 \rangle$ = 0.49
n = 1, $\langle X^2 \rangle$ = 1.50
n = 2, $\langle X^2 \rangle$ = 2.50
n = 3, $\langle X^2 \rangle$ = 3.49
n = 4, $\langle X^2 \rangle$ = 4.49
n = 5, $\langle X^2 \rangle$ = 5.49
n = 6, $\langle X^2 \rangle$ = 6.50
n = 7, $\langle X^2 \rangle$ = 7.50
n = 8, $\langle X^2 \rangle$ = 8.49
n = 9, $\langle X^2 \rangle$ = 9.49
n = 10, $\langle X^2 \rangle$ = 10.49

These results demonstrate that the potential energy increases linearly with the energy level n, as expected from quantum mechanics. Specifically, the expectation value $\langle X^2 \rangle$ for a given state n closely follows the theoretical relation $\langle X^2 \rangle \approx n + \frac{1}{2}$. This linear trend confirms the increasing spread of the wavefunction as the energy level increases, which corresponds to a broader range of possible particle positions. The consistency of the results across multiple energy levels indicates that the integration was performed accurately, with negligible numerical errors. The use of Gaussian quadrature was critical in evaluating this integral, as it ensured accurate handling of the infinite integration range and the oscillatory nature of the wavefunctions.

2. Relativistic Particle on a Spring

In this question, we are going to investigate the motion of a particle attached to a spring in both classical and relativistic regimes. The transition from one regime to the other is analyzed by calculating the period T of oscillation for varying amplitudes. Gaussian quadrature was used to integrate the equation of motion, and the results were compared with classical and relativistic limits.

a) Gaussian Quadrature for Period Calculation

The initial assumptions are $x_0 = 0.01(m), k = 12.0(N/m), c = 3.0 \times 10^8(m/s)$, and $m = 1.0(kg)$. Gaussian quadrature was applied to calculate the period T for $(N = 8)$ and $(N = 16)$ sample points, yielding times of 1.73 and 1.77 seconds, respectively. The fractional error between these two results was approximately. This error shows how increasing the number of sample points improves the precision of the integration, but even with fewer points, the results remain close to the true value.

b) Integrand and Weighted Values Plots

In this part, we analyze the behaviour of the integrand and its weighted values for Gaussian quadrature by plotting the expressions $4/g(x_k)$ and $4w_k/g(x_k)$, where w_k are the Gaussian quadrature weights, and $g(x_k)$ represents the function defining the particle's velocity. The integrand values for both $N = 8$ and $N = 16$ sample points were plotted to investigate how they behave as the upper integration limit x_0 is approached.

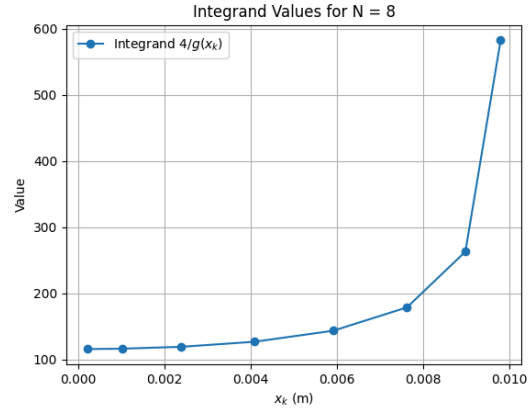

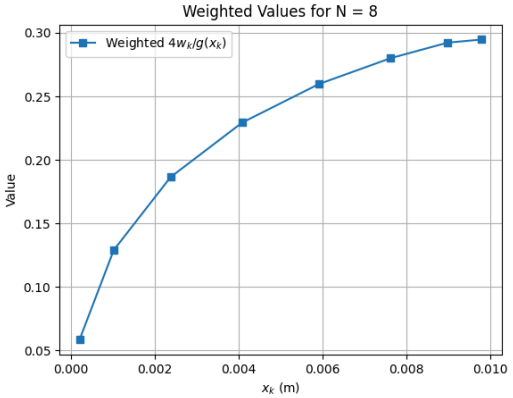

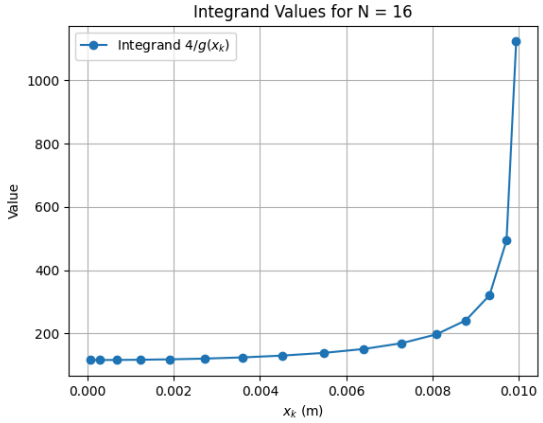

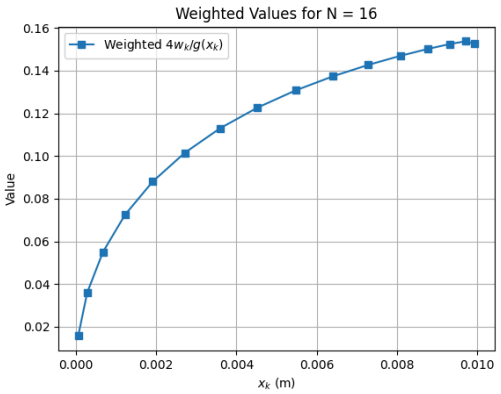

The integrand plots for $N = 8$ and $N = 16$ show that the values of $4/g(x_k)$ increase rapidly as x_k nears the upper limit of integration. This behaviour reflects the non-linear nature of the particle's velocity as it oscillates along the spring. As the amplitude x_0 approaches the limit of integration, the values of the integrand rise significantly, indicating that the system transitions into a regime where relativistic effects become more pronounced.

From weighted values plots for $4w_k/g(x_k)$ demonstrate how the weights w_k help balance the rapidly increasing integrand values, ensuring numerical stability during integration. As x_k nears the upper limit, the weighted values stabilize and grow less dramatically compared to the raw integrand. This suggests that Gaussian quadrature is effectively handling the sharp increase in the integrand, ensuring accurate numerical results.

From these plots, it is clear that the integrand values increase sharply as the particle approaches the maximum displacement x_0. The stabilization of the weighted values suggests that Gaussian quadrature weights are crucial for accurately evaluating the integral despite the rapid rise in the integrand. However, this rapid growth near the upper limit introduces some numerical challenges, which can affect the precision of the integral. This behaviour explains why higher sample points, such as $N = 16$, produce more accurate results compared to lower values like $N = 8$, as they provide finer sampling near the critical points of the integration range.

c) Period as a Function of Amplitude

This part explores how the period T of the relativistic particle on a spring changes as the amplitude x_0 varies from a small displacement to large values where relativistic effects dominate. Using Gaussian quadrature with $N = 16$ sample points, we calculated the period T for a range of amplitudes from $x_0 = 1\,\mathrm{m}$ to $x_0 = 10x_c$, where $x_c$is the critical displacement at which the particle reaches the speed of light c. The critical displacement is given by:

$$x_c = c\sqrt{\frac{m}{k}}$$

where m is the mass of the particle, k is the spring constant, and c is the speed of light. As the amplitude x_0 increases, the system transitions from the classical regime, where the period is constant, to the relativistic regime, where the period increases linearly with the amplitude.

The plot below shows the computed period T as a function of amplitude x_0, alongside the classical and relativistic limits. For small amplitudes, the period approaches the classical limit, represented by the horizontal red line at $T = 2\pi\sqrt{m/k}$. This constant period reflects the fact that in the classical regime, the oscillation is governed by Hooke's law, with no significant relativistic effects. As the amplitude x_0 increases, the particle's velocity approaches the speed of light, causing the period to increase linearly with x_0. This behavior matches the relativistic limit, represented by the black dashed line, where $T = 4x_0/c$.

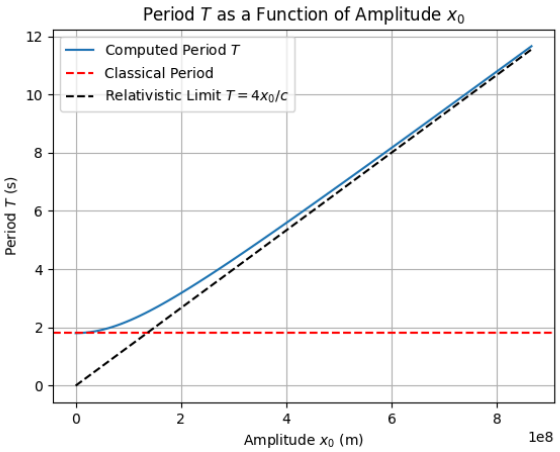

The plot clearly shows the transition between the classical and relativistic regimes. For small values of x_0, the period remains nearly constant, confirming that the system behaves as expected under classical mechanics. However, as x_0 increases beyond several multiples of x_c, the period T begins to rise steadily, reflecting the increasing difficulty of accelerating the particle as its velocity approaches the speed of light. This linear growth aligns with the relativistic limit, where the period depends directly on the displacement. The ability to compute the period across such a wide range of

amplitudes demonstrates the versatility of Gaussian quadrature. The gradual convergence of the numerical results with the classical and relativistic limits further validates the accuracy of the method.

3. Numerical Differentiation

In this section, numerical differentiation techniques were applied to the function $f(x) = e^{-x^2}$. Two finite difference methods, central and forward difference, were used to approximate derivatives, and the results were compared with analytical solutions. Error analysis was performed to understand the behaviour of numerical methods at different step sizes.

a) Central Difference Approximation

Using the central difference approximation:

$$f'(x) \approx \frac{f(x + h/2) - f(x - h/2)}{h} \equiv \Delta_h f|_x$$

where we have defined $\Delta_h f|_x$ as a central difference operator applied to f at x for a given interval h. The derivative of $f(x) = e^{-x^2}$ was computed at $x = 0.5$ by a factor of 10 step sizes h ranging from $10^{-16} \rightarrow 10^0$. The results showed convergence towards the analytical values as h approached an optimal range.

b) Analytical derivative and Minimum Error

The analytical derivative of the function $f(x) = e^{-x^2}$ at $x = 0.5$ is:

$f'(x) = -2xe^{-x^2}$ Substituting \(x = 0.5\), we get:

$$f'(0.5) = -2(0.5)e^{-0.5^2} = -0.7788$$

Using this analytical value as the ground truth, we calculated the absolute value of the relative error for each numerical derivative obtained using the central difference approximation across different step sizes h. The smallest relative error was found to be approximately 1.8182×10^{-11} at the 11th step when $h \approx 10^{-6}$.

This behavior closely aligns with the theoretical expectations discussed in Section 5.10 of the textbook. As described, the optimal step size minimizes the competing effects of truncation error and roundoff error. Truncation errors occur when h is large, leading to an imprecise approximation of the derivative. Conversely, roundoff errors dominate when h is too small due to limitations in floating-point precision (with machine precision constant $C \approx 10^{-16}$). The balance between these two types of error leads to an optimal $h \approx 10^{-8}$, which is somewhat consistent with what was observed in the results.

c) Forward Difference Approximation

The forward difference approximation was used to calculate the derivative of $f(x) = e^{-x^2}$ at $x = 0.5$. The formula for the forward difference approximation is:

$$f'(x) \approx \frac{f(x+h) - f(x)}{h}$$

In this method, the derivative is approximated by evaluating the function at $x + h$ and x, rather than symmetrically around x as in the central difference method. The minimum relative error using the forward difference method was found to be approximately 9.5693×10^{-9} at the 9th step when $h \approx 10^{-8}$.

Although the forward difference approximation provides reasonably accurate results, the errors are noticeably larger compared to the central difference method. As explained in Section 5.10 of the textbook, this is due to the inherent asymmetry of the forward difference method, which amplifies approximation errors. Additionally, forward difference is more sensitive to roundoff errors for small h, as it relies on subtracting two nearly equal numbers, which leads to larger relative errors.

The results align with the theoretical discussion in the textbook. The optimal h found for the forward difference method is larger than that for the central difference method, which is expected. Since the forward difference is a first-order method (with an error proportional to h), it requires a larger step size to mitigate the effects of roundoff error. In contrast, the central difference method, being second-order, provides more accurate results even with smaller step sizes.

d) Error Analysis Plot

The plot of relative errors for both central and forward difference methods reveals that the central difference method performs better across most step sizes. However, at very small h, both methods suffer from roundoff errors.

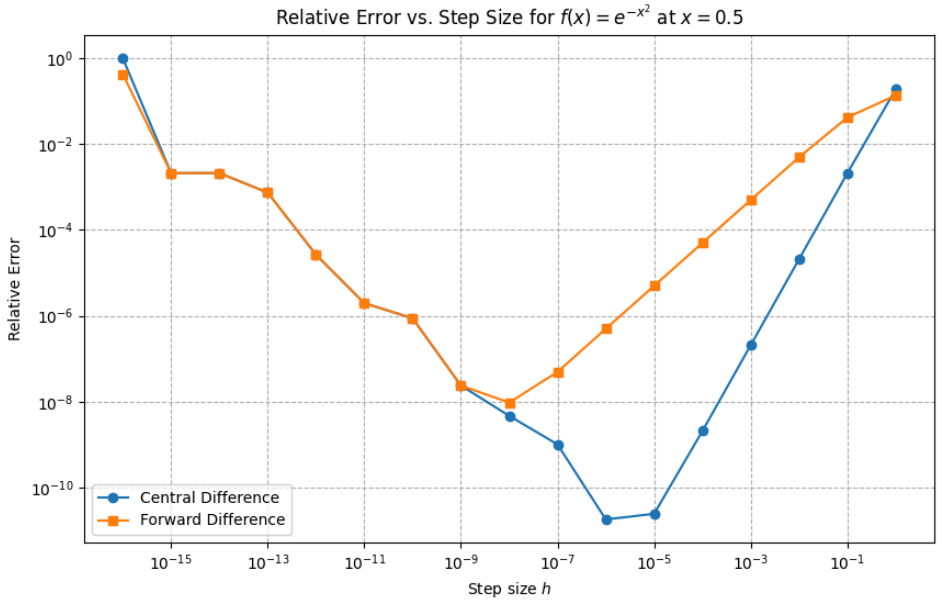

The central difference method consistently outperforms the forward difference method across most step sizes. This superior performance is due to the fact that the central difference method has a second-order error term $O(h^2)$, meaning the approximation error decreases quadratically as h becomes smaller. In contrast, the forward difference method has only a first-order error term $O(h)$, which makes it less accurate overall.

The plot also highlights the importance of choosing the right numerical method for differentiation. While the central difference method provides greater accuracy, it is more computationally expensive because it requires evaluating the function at two points around x. On the other hand, the forward difference method is computationally cheaper but less accurate, particularly for small step sizes, due to its sensitivity to roundoff errors.

e) Error behaviour at Extreme h Values

At small step sizes, the error curves for both methods increase sharply. This increase is caused by roundoff errors resulting from the limitations of floating-point arithmetic, where the subtraction of nearly equal values introduces significant precision loss. Therefore at very small h, roundoff errors become significant, as floating-point precision is insufficient to capture the small differences involved in the calculation.

At large step sizes, truncation errors dominate. These errors occur because the derivative approximation becomes less accurate as the interval h becomes too large, causing the approximation to deviate from the true slope of the function. The plot confirms this behavior, as the error increases steadily for both methods when h is large. We can conclude that at large h, truncation errors dominate, leading to inaccurate results due to the approximation's coarseness

f) Higher-Order Derivatives of $g(x) = e^{2x}$

Using the central difference method with $h = 10^{-6}$, the first five derivatives of $g(x) = e^{2x}$ were calculated at $x = 0$. The numerical results closely matched the analytical values until the second derivative:

First Derivative: $RelativeError = 2.68 \times 10^{-11}$
Second Derivative: $RelativeError = 5.63 \times 10^{-6}$
Third Derivative: $RelativeError = 1.29 \times 10^{1}$
Fourth Derivative: $RelativeError = 6.94 \times 10^{6}$
Fifth Derivative: $RelativeError = 6.94 \times 10^{12}$

The first two derivatives show agreement with their analytical values, with small relative errors. However, starting from the third derivative, the error increases significantly, reaching a magnitude on the order of 10^{12} by the fifth derivative. This behaviour indicates that higher-order derivatives become increasingly prone to numerical instability due to both truncation and roundoff errors. The large errors for higher derivatives arise from repeated applications of the central difference operator, amplifying small inaccuracies in each step and illustrating the limitations of finite difference methods for computing higher-order derivatives.